

VL-GPT: A Generative Pre-trained Transformer for Vision and Language Understanding and Generation

Jinguo Zhu^{1*} Xiaohan Ding^{2*} Yixiao Ge^{2,3} Yuying Ge²
Sijie Zhao² Hengshuang Zhao⁴ Xiaohua Wang¹ Ying Shan^{2,3}✉
¹ Xi'an Jiaotong University ² Tencent AI Lab
³ ARC Lab, Tencent PCG ⁴ The University of Hong Kong

Abstract

In this work, we introduce Vision-Language Generative Pre-trained Transformer (VL-GPT), a transformer model proficient at concurrently perceiving and generating visual and linguistic data. VL-GPT achieves a unified pre-training approach for both image and text modalities by employing a straightforward auto-regressive objective, thereby enabling the model to process image and text as seamlessly as a language model processes text. To accomplish this, we initially propose a novel image tokenizer-detokenizer framework for visual data, specifically designed to transform raw images into a sequence of continuous embeddings and reconstruct them accordingly. In combination with the existing text tokenizer and detokenizer, this framework allows for the encoding of interleaved image-text data into a multimodal sequence, which can subsequently be fed into the transformer model. Consequently, VL-GPT can perform large-scale pre-training on multimodal corpora utilizing a unified auto-regressive objective (i.e., next-token prediction). Upon completion of pre-training, VL-GPT exhibits remarkable zero-shot and few-shot performance across a diverse range of vision and language understanding and generation tasks, including image captioning, visual question answering, text-to-image generation, and more. Additionally, the pre-trained model retrains in-context learning capabilities when provided with multimodal prompts. We further conduct instruction tuning on our VL-GPT, highlighting its exceptional potential for multimodal assistance.

1. Introduction

Driven by the remarkable success of large language models (LLMs) in the field of natural language processing

*Equal contribution. This work is done when Jinguo Zhu is an intern at Tencent AI Lab. The source code and model weights shall be released at <https://github.com/AI-Lab-CVC/VL-GPT>. ✉Corresponding author.

(NLP) [40, 41, 54], there has been a surge of interest within multimodal community to develop large vision-language (VL) models. One of the promising approaches, exemplified by Flamingo [1], BLIP2 [24], LLAVA [25], have explored how to build large VL models based on powerful pre-trained LLMs. These studies typically adopted a similar architecture: a pre-trained image encoder and an LLM are connected via a trainable connection module, which aligns the image feature and text embeddings, thereby enabling language models to accept images and text as inputs and generate a text sequence.

To expand the capabilities of generating image in a multimodal context, certain efforts, e.g., Visual ChatGPT [47], attempt to connect LLMs with image generation tools in a cascaded pipeline by transferring text messages, which inevitably introduce instability and noise. Alternatively, another line of research achieves it by optimizing models in an end-to-end manner [9, 18, 23, 30, 48]. By aligning the output space with the image diffusion models, VL models can not only perceive but also generate images and text.

A crucial characteristic of large language models is auto-regressive modeling [31], i.e., predicting next token, which facilitates language understanding and generation in a unified manner. However, in the aforementioned studies, the inconsistency of image embeddings between LLM’s input and output sides compels the model to treat input images and generated images differently, resulting in separate modeling for image understanding and generation. Meanwhile, this discrepancy also obstructs the implementation of auto-regressive training loss on image embeddings.

In this study, we introduce VL-GPT, a large vision-language generative pre-trained transformer that enables the unified training of both visual and linguistic data using an auto-regressive objective, as depicted in Fig. 1. To achieve this, we propose an image tokenizer-detokenizer framework for the conversion between raw image pixels and continuous visual embeddings, analogous to the role of the text tokenization [19, 43] in language models. The framework

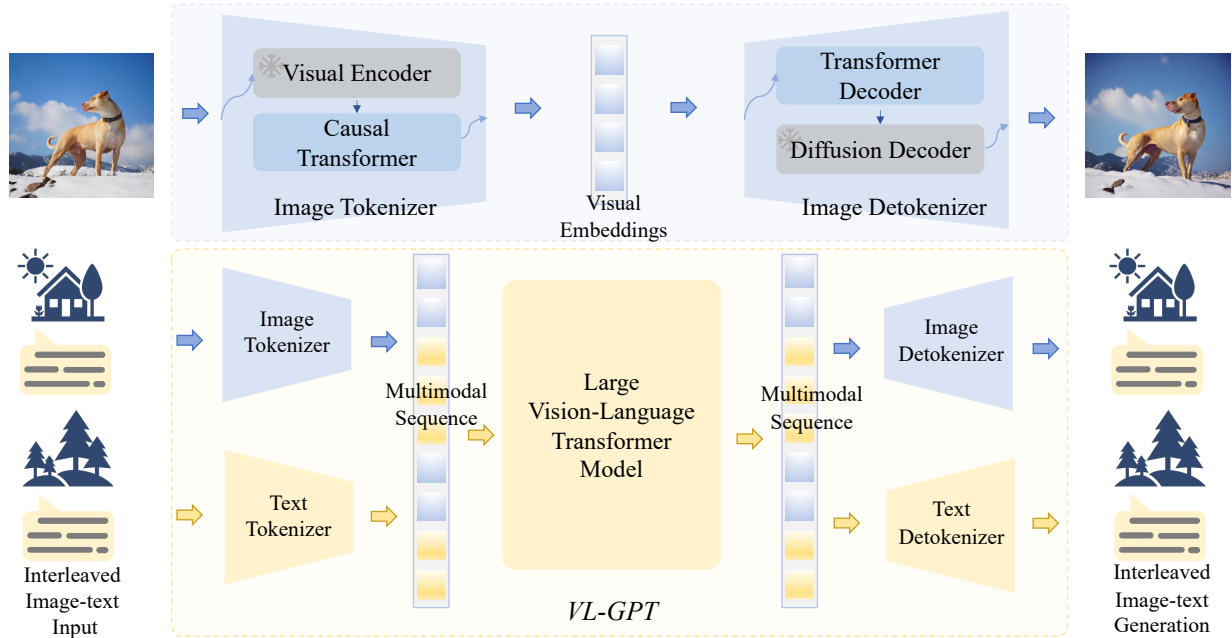


Figure 1. Overview of our proposed approach. The upper part delineates the image tokenizer-detokenizer framework, designed for encoding images into continuous visual embeddings and reconstructing them in the pixel space. The lower part demonstrates the implementation of our VL-GPT, where interleaved image-text data are encoded into multimodal sequence using image and text tokenizers, subsequently processed by a transformer model auto-regressively. The image and text detokenizers are employed for generating respective outputs.

comprises an image tokenizer and an image detokenizer, where the tokenizer encodes raw images into a sequence of continuous visual embeddings, and the detokenizer decodes the continuous embeddings into pixel space. To obtain visual continuous embeddings that are rich in both image details and semantic information, we employ the image embeddings and their corresponding caption embeddings extracted by pre-trained encoders (*i.e.*, CLIP [32]) as the supervision for training of the framework. Furthermore, the efficiency of the framework training is enhanced through weight initialization from pre-trained image encoders and high-quality image diffusion models.

By employing the image tokenizer-detokenizer framework, visual embeddings can achieve consistency on both the input and output sides of the transformer model. Consequently, interleaved image-text data can be trained in a unified auto-regressive manner. Specifically, the image tokenizer and the existing text tokenizer (*i.e.*, BPE tokenizer [43]) first convert the image and text into a multimodal sequence consisting of interleaved continuous visual embeddings and discrete text tokens. The transformer can then be trained to predict the next embedding or token in this multimodal sequence, employing mean squared error (MSE) loss for continuous visual embeddings and cross-entropy loss for discrete text tokens. Contrary to previous works [9, 18, 30, 48], all embeddings in the multimodal sequence can receive supervision from the auto-regressive loss. During the generation stage, visual embeddings and

text tokens can be generated auto-regressively without distinction, and subsequently decoded into raw images and text by the image detokenizer and text detokenizer, respectively.

Owing to the unified modeling, the pre-training of the VL model can be conducted on large-scale image-text pairs and interleaved image-text data. Upon completion of pre-training, the model is capable of perceiving arbitrary multimodal input and generating responses varying in modalities (*e.g.*, text, images or their interleaved contents), allowing it to generalize to a wide range of vision and language understanding and generation tasks in a zero-shot or few-shot manner. Moreover, the pre-trained model exhibits appealing emergent properties for multimodal in-context learning, as it can effectively tackle new unseen tasks when provided with multimodal prompts. The VL generative pre-trained transformer model, referred to as VL-GPT, holds the potential to serve as a powerful foundation model for the multimodal community, similar to the role of GPT family [4, 29] in NLP. Our contributions are summarized as follows:

- We propose an image tokenizer-detokenizer framework to convert images into continuous embeddings and reconstruct them, while exploring effective training methods for this framework.

Through efficient training that requires an affordable computational cost, the image tokenizer and detokenizer can effectively retain both semantic information and pixel details of the original image.

- We introduce VL-GPT, a generative pre-trained trans-

former model for vision and language (VL) understanding and generation tasks. The model can be pre-trained on large-scale multimodal corpora in a unified auto-regressive manner, *i.e.*, predicting the next token in a multimodal sequence containing continuous visual embeddings and discrete text tokens without any discrimination.

- VL-GPT exhibits competitive performance on various VL understanding and generation benchmarks under zero-shot and few-shot settings, including image captioning, visual question answering, and text-to-image generation. It also demonstrates an appealing multimodal in-context learning ability when provided with multimodal prompts. Furthermore, it shows promising potential to serve as a general multimodal assistant through instruction tuning.

2. Related Work

Multimodal Pre-training in the Pre-LLM Era. Prior research efforts primarily concentrated on model architecture to facilitate the fusion and interaction of cross-model data [6, 50, 52]. The success of transformers in language models [42] and ViT [10] inspired the development of unified multi-modal modeling [27, 44]. Although images and language can be processed by a unified model with shared parameters, they often have distinct training objectives. It is worth mentioning that the BEiT series [2, 45] successfully adapted the masked language modeling objective from BERT [8] to vision and multimodal pre-training.

Multimodal Pre-training in the LLM Era. Building upon pre-trained large language models (LLMs) [33, 40, 41, 54], recent studies have effectively developed multimodal language models capable of processing image and text inputs to generate text outputs [1, 22, 24, 25, 56]. Another challenge for large multimodal models is generating multimodal content beyond language. Several efforts, such as Visual ChatGPT [47] and HuggingGPT [38], have achieved this by connecting LLMs with other generation tools within an LLM integration framework, *e.g.*, LangChain. However, these systems exhibit instability and limited room for further optimization. To enable LLMs to generate images with optimization, M-VADER [46] aligns the semantic consistency between an LLM and a diffusion decoder by training them on image-text pair data. GILL [18] achieves more complex interleaved image-text generation by mapping the embedding spaces of the LLM to text-to-image generation models. NExT-GPT [48] extends this concept to additional modalities, such as audio and video. DreamLLM [9] facilitates passing the differential gradient from image diffusion models to language models, enabling the generation of free-form interleaved content. Following similar methods, Kosmos-G [30] enhances the fidelity of generated images in context through a compositional instruction tuning task.

In contrast to our VL-GPT, these studies mainly focus on

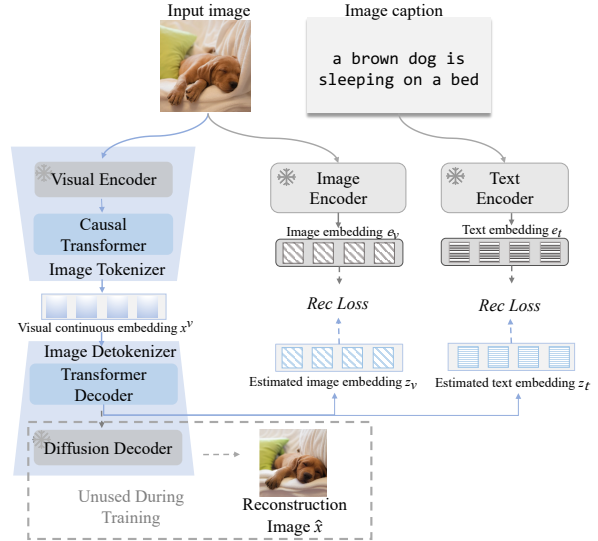


Figure 2. The training scheme of our image tokenizer-detokenizer framework, which is supervised by the frozen image and text encoders of our adopted pre-trained image diffusion model. Only the causal transformer in tokenizer and the transformer decoder in detokenizer necessitate training, while the diffusion decoder in detokenizer remains unused during training.

leveraging existing LLMs and exploring the integration of current image encoders and image generation models into LLMs. However, these methods do not achieve unified modeling for images and language, nor unified modeling for image understanding and generation. For instance, special queries are typically needed to encapsulate the context information for image generation, but they are deemed unnecessary when images serve as input for LLMs. Moreover, applying an auto-regressive training objective on visual embeddings is challenging due to the inconsistency of image embedding space. Consequently, these approaches are limited in expanding the scalable pre-training paradigm for the GPT family, *i.e.*, next-token prediction, to large vision-language models on web-scale multimodal corpora.

Recently, Emu [39] proposes a multimodal pre-trained model that enables the auto-regressive training for both visual and text embeddings. However, it requires a costly second-stage fine-tuning of the Stable Diffusion [35] to convert the visual embeddings into pixel space. In contrast, our method utilizes a novel image tokenizer-detokenizer framework that can fully leverage a pre-trained image diffusion model (see Fig. 2). This approach not only simplifies the process but also enhances training efficiency. Similar to our approach, SEED [11] initially trains an image tokenizer, followed by a multi-modal training. Nevertheless, its tokenizer encodes images into discrete tokens via quantization operations, potentially losing partial image information. In contrast, our tokenizer converts images into continuous visual embeddings, preserving both semantic information and appearance details, resulting in improved performance across

diverse benchmarks.

3. Method

As illustrated in Fig. 1, the implementation of our VL-GPT can be separated into two consecutive stages. In the first stage, we learn an image tokenizer-detokenizer framework, capable of encoding images into continuous visual embeddings and decoding them back. The second stage is the pre-training and instruction tuning of our VL-GPT, which facilitates a unified modeling approach for vision and language understanding and generation. In the following sections, we will provide a detailed description of these two stages.

3.1. Image Tokenizer-Detokenizer Framework

To implement an auto-regressive training objective on visual embeddings and text tokens concurrently, we develop an image tokenizer-detokenizer framework for vision-language models. The framework, inspired by text tokenizers utilized in language models [43], can realize bi-directional conversion between original images and continuous visual embeddings, thereby enabling the transformer model to process vision data akin to processing text data.

Architecture The overall architecture of our image tokenizer-detokenizer framework is depicted in Fig. 1. It comprises two primary components: a tokenizer \mathcal{E} responsible for encoding the image into continuous visual embeddings, and a detokenizer \mathcal{D} dedicated to decoding the visual embeddings back to raw images.

Formally, the image tokenizer \mathcal{E} employs an image encoder (e.g., ViT [10]) to extract spatial patched features \mathbf{x}^p from the given image \mathbf{x} . Subsequently, a standard decoder-only causal transformer is utilized to convert the patched features \mathbf{x}^p to 1D (one-dimensional) visual embeddings $\mathbf{x}^v \in \mathbb{R}^{N \times d}$, where N represents the number of visual embeddings, and d denotes the embedding dimension. The 1D continuous visual embeddings \mathbf{x}^v serve as input embeddings to our vision-language model, analogous to word tokens in language models.

Inspired by current image diffusion models with excellent performance and accessibility [34, 35, 49], our image detokenizer \mathcal{D} learns a latent diffusion model to decode visual embeddings \mathbf{x}^v into images. Specifically, a transformer decoder is employed to estimate condition embedding \mathbf{z} from \mathbf{x}^v . Then a diffusion decoder, initialized from a pre-trained image diffusion models, can generate images $\hat{\mathbf{x}}$ based on estimated condition embedding \mathbf{z} .

Training Despite the initialization with pre-trained models, conducting a full-scale end-to-end optimization of the image tokenizer and detokenizer demands large-scale data and considerable training costs. To pursue efficient training, we opt to train the transformer decoder in image detokenizer to estimate the condition embedding utilized for the diffu-

sion decoders, as illustrated in Fig. 2. Notably, the diffusion decoder, including its U-Net and VAE modules, is not employed during framework training, substantially enhancing the efficiency of training procedure.

As Fig. 2 shows, the training objective of our framework aims to concurrently reconstruct the image condition embedding e_v and text condition embedding e_t . This design distinguishes our framework from previous works [11, 18, 48], which only align their intermediate outputs with text embedding produced by the text encoder of the diffusion model. Specifically, we optimize the framework by minimizing the following loss function (with weight λ_1 and λ_2):

$$L(\mathbf{z}) = \lambda_1 * \text{MSE}(z_v, e_v) + \lambda_2 * \text{MSE}(z_t, e_t) \quad (1)$$

where $\text{MSE}(\cdot)$ denotes the mean squared error loss, and z_v and z_t represent the estimated image condition embedding and estimated text condition embedding, respectively. During inference, both types of condition embedding contribute collectively to generate images. Our image tokenizer-detokenizer framework can also work when reconstructing only image condition embedding (if $\lambda_2=0$) or only text condition embedding (if $\lambda_1=0$). Moreover, the training for estimating image embedding only requires visual data, which is more training-friendly than estimating text embedding. However, our experiments in Sec. 4.5 reveal that these two types of embedding complement each other: text embedding contain rich semantic information while image embedding effectively persevere image details.

3.2. VL-GPT

VL-GPT aims to process the vision and language understanding and generation within a single transformer model in a unified way, similar to GPT handles language tasks. It is capable of perceiving the interleaved multi-modal data and generating content across various modalities. By employing unified modeling, our VL-GPT can conduct auto-regressive pre-training on web-scale multimodal corpora, thereby holding the potential to serve as a powerful foundation model in the multimodal research community.

Architecture As depicted at the bottom of Fig. 1, our VL-GPT comprises five components: a large vision-language transformer model \mathcal{M} , an image tokenizer \mathcal{E}_v , a text tokenizer \mathcal{E}_t , an image detokenizer \mathcal{D}_v and a text detokenizer \mathcal{D}_t . In comparison to a language model, VL-GPT incorporates additional image tokenizer and image detokenizer elements.

Given any interleaved image-text data, the image tokenizer and the text tokenizer initially encode them into a multimodal sequence. More specifically, the image tokenizer \mathcal{E}_v converts each image into N continuous visual embeddings \mathbf{x}^v . Additionally, two special tokens [IMG] and [/IMG] are appended at the beginning and end of the visual embeddings, respectively. The visual embeddings are

then combined with the discrete text tokens encoded by the text tokenizer \mathcal{E}_t to form an interleaved multimodal sequence $\mathbf{v} = (v_1, v_2, \dots, v_n)$, where v_i can be either a discrete text token or a continuous visual embedding. The multimodal sequence \mathbf{v} is then fed into the large VL model \mathcal{M} for unified auto-regressive modeling.

The output embedding $\mathcal{M}(v_i)$ can be flexibly transformed into a text embedding through a language modeling head for the predefined vocabulary or into a visual embedding with a separate regression head. During training, the selection of the transformed head depends on whether the target for the current embedding is a text token or a visual embedding. During inference, if [IMG] is predicted, the visual regression head will be utilized to transform output embeddings in the subsequent N prediction; otherwise, the language modeling head will be used. The prediction embeddings are subsequently decoded to raw images or text via the image detokenizer \mathcal{D}_v or the text detokenizer \mathcal{D}_t .

Multimodal Pre-training. Benefiting from the unified modeling of both visual and text embeddings, we can apply the unsupervised pre-training paradigm of GPT [31] to our VL-GPT on a large corpus of multimodal data with minimal modifications.

Given an interleaved multimodal sequence $\mathbf{v} = (v_1, v_2, \dots, v_n)$ in a large-scale corpora, we employ the standard auto-regressive modeling objective in language models to maximize the following likelihood:

$$L(\mathbf{v}) = \sum_i^n \log P(v_i | v_1, v_2, \dots, v_{i-1}; \Theta) \quad (2)$$

where Θ represents the parameters of our VL-GPT. We apply cross-entropy loss with a language modeling head on the discrete text tokens and utilize MSE loss with a regression head for continuous visual embeddings.

Instruction Tuning To enhance the ability of the pre-trained VL-GPT to follow human instructions faithfully and generate multimodal contents creatively, we perform further instruction tuning of VL-GPT using publicly available instruction-tuning datasets. Briefly, the data from these datasets will be restructured into a conversational format, *i.e.*, pairs of multimodal human instructions and their responses for single or multiple rounds, and subsequently employed for model tuning in a manner similar to the pre-training corpora. A minor deviation from pre-training process is that the training objective will be applied exclusively to the embeddings tokenized from answer responses.

4. Experiments

The training of our VL-GPT consists of three phases: training for the tokenizer-detokenizer framework, unified multimodal pre-training for the vision-language transformer model, and instruction tuning for the pre-trained VL-GPT.



Figure 3. Reconstruction images of our image tokenizer-detokenizer framework by utilizing image condition embedding (z_v), or text condition embedding (z_t), or both types of condition embedding (z_v+z_t). More examples are included in the appendix.

Model	COCO	Flickr30k
GILL [18]	67.45	65.16
SD v1.5 [35]	68.43	65.40
SEED [11]	68.23	65.22
unCLIP [34]	79.30	79.55
Our tokenizer-detokenizer	80.22	79.14

Table 1. Evaluation of image reconstruction with CLIP similarity.

4.1. Datasets

Publicly available datasets are utilized for different phrase of the VL-GPT training. The image tokenizer-detokenizer framework is trained on image-text pairs from CC3M [37], LAION-Aesthetics [20], and LAION-COCO [36]. During the unified multimodal pre-training of VL-GPT, a combination of paired and interleaved image-text data is employed. The image-text pairs remain consistent with the preview phase, while the interleaved image-text sequences are acquired from Multimodal-C4 (MMC4) [57] and OBELICS [21]. We adopt similar preprocessing techniques for interleaved data implemented in Flamingo [1]. For each document, a maximum of 5 images and their associated captions are randomly sampled to construct a subsequence with a token length of up to 512. Additionally, for paired and interleaved image-text data, each image is randomly placed before or after its corresponding caption. For the instruction tuning of VL-GPT, a compositional instruction tuning dataset is constructed from various sources, encompassing conversational data from LLAVA [25] and SVIT [55], image-text pair data from COCO Caption [5], and image editing data from InstructPix2Pix [3] and Magicbrush [53]. These datasets are restructured into a conver-

Models	Image-Text understanding						Text-to-image generations
	COCO	VQAv2	GQA	OKVQA	VizWiz	VisDial	COCO FID (\downarrow)
► VL Understanding or generation Models							
MetaLM [14]	82.2	41.1	-	11.4	-	-	-
Kosmos-1 [16]	84.7	51.0	-	-	29.2	-	-
Flamingo-9B [¶] [1]	79.4	51.8	-	44.7	28.8	48.0	-
SD v1.5 [35]	-	-	-	-	-	-	9.22
► Unified VL understanding and generation Pre-trained Models							
GILL [18]	-	-	-	-	-	-	12.2
Kosmos-G-1.9B [30]	-	-	-	-	-	-	10.99
SEED-OPT _{2.7B} [11]	119.0	42.8	28.8	-	-	-	-
Emu [39]	112.4	52.0	-	38.2	34.2	47.4	11.66
Emu [†] [39]	-	52.9	-	42.8	34.4	47.8	-
VL-GPT	116.4	51.7	34.6	35.8	34.7	49.9	12.25
VL-GPT [†]	119.2	55.3	38.1	41.5	35.2	49.6	-
► Unified VL understanding and generation Models with Instruction-tuning or Fine-tuning							
CM3Leon-7B [51]	61.6	47.6	-	23.8	37.6	22.6	10.82
Emu-1 [39]	-	57.5	-	46.2	38.1	50.1	-
NExT-GPT [§] [48]	156.7	-	-	-	-	-	11.28
DreamLLM-7B [9]	115.4	56.6	-	44.3	38.1	-	8.46
VL-GPT-I	133.7	67.2	51.5	50.3	38.9	51.8	11.53

Table 2. Evaluation comparison between our VL-GPT and other models. [†] denotes that the zero-shot prompt is built by sampling two task-specific examples with their associated images removed. [§] represents that the dataset employed for instruction tuning is private.

sational format using the template provided in the appendix. For further details regarding preprocessing and construction of our training dataset, please refer to the appendix as well.

4.2. Training setup

To efficiently train the image tokenizer-detokenizer framework, the visual encoder in the image tokenizer and the diffusion decoder in the image detokenizer are initialized with CLIP-L image encoder [32] and IP-Adapter [49], respectively. Moreover, these two modules remain frozen throughout the entire training, and only the causal transformer and the transformer decoder necessitate optimization. Unless specified otherwise, the weight coefficients λ_1 and λ_2 in Eq. 1 are assigned a value of 1.0 during both training and evaluation. The AdamW optimizer [26] is employed for training, with a learning rate of $2e-4$ and a cosine schedule. The framework is trained using a total batch size of 1024 on 8 NVIDIA 40G-A100 GPUs for 10,000 iterations.

For the multimodal pre-training of our VL-GPT, the pre-trained LLaMA 7B [40], its text tokenizer, and its text detokenizer are integrated with our trained image tokenizer and detokenizer to establish the VL-GPT model with a total of 7.5 billion parameters. LoRA [15] module is incorporated into the LLaMA model, resulting in relatively low demand for computational resources. AdamW optimizer is also utilized with a learning rate of $2e-4$. The multimodal pre-training is conducted with a batch size of 4096 on 32 GPUs for 20,000 iterations. Instruction tuning is performed on the pre-trained VL-GPT, adopting similar training settings used during pre-training. LoRA is also employed, and the learning rate is reduced to $5e-5$. The model is trained for 10,000

iterations with batch size of 512 on 4 GPUs. Additional training settings are included in the appendix.

4.3. Image Tokenizer and Detokenizer Performance

The image tokenizer-detokenizer framework is designed to convert images between pixel space and continuous visual embeddings. To assess its effectiveness, we employ the method of calculating the CLIP similarity as the evaluation metric for our framework, as implemented in SEED [11]. As demonstrated in Tab. 1, our framework achieves notably superior semantic consistency compared to SEED, which utilized quantized visual tokens.

Furthermore, we present visualizations of the reconstructed images generated by our framework in Fig. 3. By estimating both image condition embedding and text condition embedding and utilizing them to guide the generation process of diffusion decoder, our image detokenizer is capable of generating images with high consistency in terms of spatial appearance and semantic information.

4.4. Evaluation of our VL-GPT

Benchmark Performance We first evaluate the zero-shot performance of VL-GPT on a variety of vision-language tasks, including image captioning on MSCOCO [5], visual question answering on VQAv2 [12], GQA [17], OKVQA [28], and VizWiz [13], visual dialog on VisDial [7], and text-to-image generation on MSCOCO. Comprehensive details regarding these benchmarks and their metrics can be found in the appendix. As results in Tab. 2 indicate, VL-GPT achieves competitive performance on

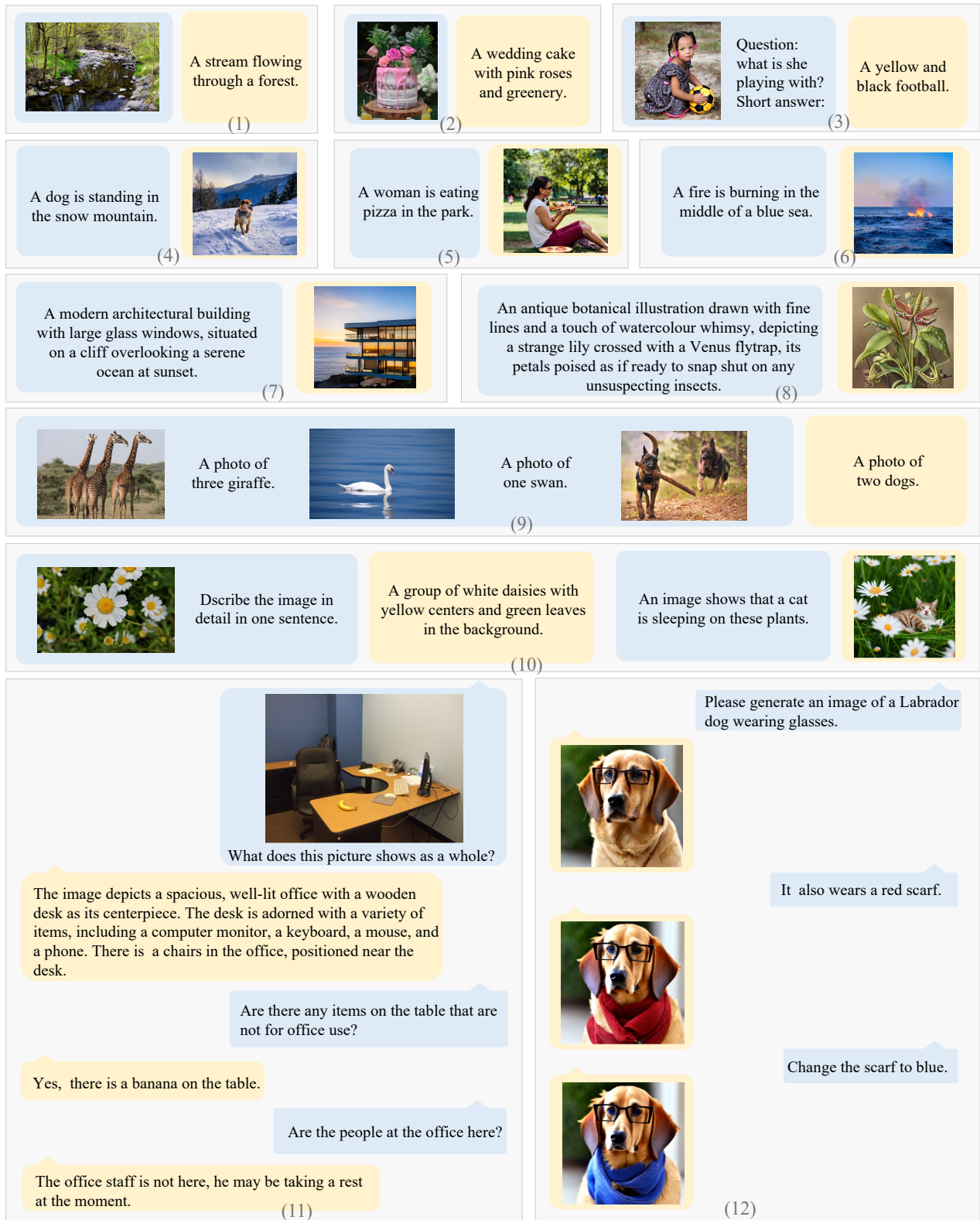


Figure 4. Illustrative samples of our VL-GPT across various vision and language understanding and generation tasks. These tasks encompass: (1)-(2) image captioning, (3) visual question answering (VQA), (4)-(8) text-to-image generation, (9)-(10) multimodal in-context generation, and (11)-(12) multimodal dialogue. Examples (1)-(10) are generated by our pre-trained VL-GPT, while (11)-(12) are produced by our instruction-tuned VL-GPT. Blue boxes represent multimodal inputs and yellow boxes indicate VL-GPT outputs.

Models k	VQAv2			VizWiz		
	2	4	8	2	4	8
Kosmos-1 [16]	51.4	51.8	51.4	31.4	35.3	39.0
Flamingo-9B [1]	-	56.3	58.0	-	34.9	39.4
Emu [39]	56.4	58.4	59.0	37.8	41.3	43.9
VL-GPT	57.2	58.6	58.9	38.9	41.8	44.2

Table 3. Few-shot performance on visual question answering.

Estimation target	Reconstruction	VL-GPT	
	CLIP Similarity (\uparrow)	Captioning CIDEr (\uparrow)	Generation FID (\downarrow)
e_t	73.59	131.1	12.79
e_v	80.05	123.6	13.61
$e_t + e_v$	80.22	133.7	12.25

Table 4. Ablation of condition embedding types. Text embedding (e_t), image embedding (e_v), or their combination ($e_t + e_v$) are employed to guide the training of the tokenizer-detokenizer framework. We evaluate the effectiveness of reconstructing images and the performance of VL-GPT when adopting different image tokenizer and detokenizer.

both image-text understanding and text-to-image generation tasks, thereby validating the effectiveness of unified multimodal pre-training. Notably, VL-GPT attains an impressive CIDEr score of 116.4 or 119.2 on MSCOCO captioning without or with text-only prompts, surpassing other unified VL pre-trained models. With further instruction tuning, VL-GPT-I, the instruction-tuned VL-GPT, significantly enhances model performance, achieving the best or near-best results in all tasks.

Multimodal In-context Learning Similar to the behavior of LLMs, our VL-GPT can be prompted to address new vision-language tasks when provided with a few multimodal examples from training data composed in the multimodal prompt. To quantitatively evaluate its multimodal in-context learning capability, we examine the few-shot performance of VL-GPT when varying the number of examples in the given prompt, as shown in Tab. 3. Our VL-GPT outperforms other works under almost all few-shot setting ($k=2, 4, 8$) on two datasets for the visual question answering task. Moreover, a positive correlation is observed between the number of the examples in the given prompt and the performance on these two datasets.

Qualitative Results Fig. 4 showcases a series of generated visualizations using our VL-GPT model, encompassing various tasks such as image captioning, visual question answering, text-to-image generation, multimodal generation with in-context learning, and multimodal multi-turn dialogue. Intriguingly, VL-GPT demonstrates remarkable capabilities that are not readily assessed through existing academic benchmarks. For instance, in Fig. 4 (7-8), VL-

GPT generates highly realistic images in response to long-text prompts containing complex concepts. In Fig. 4 (10), VL-GPT exhibits the ability to generate images and texts in a flexible manner, conditioned on the provided multimodal context. Fig. 4 (11-12) illustrates the multi-turn dialogue capabilities of the instruction-tuned VL-GPT, wherein the model generates multimodal contents consistent with the existing context based on user instructions. This suggests the promising potential of the VL-GPT as a versatile and effective multimodal general assistant.

4.5. Ablation Studies

Previous studies typically generate images by converting their output into text condition embedding for image diffusion models. In contrast, our detokenizer estimates both text condition embedding and image condition embedding from visual continuous embeddings, as depicted in Sec. 3.1. The advantage of this design will be discussed next.

Fig. 3 displays the images reconstructed by our tokenizer-detokenizer using different estimated condition embedding, *i.e.*, only using image condition embedding, only using text condition embedding, or using both. These examples reveal that these two type of embedding complement each other: image embedding effectively preserve image appearance details while text embedding assists in image reconstruction, *e.g.*, determining the number of people.

As evidenced in Tab. 4, although it is feasible to train image tokenizer-detokenizer framework by estimating solely one type of condition embedding (when $\lambda_1=0$ or $\lambda_2=0$ in Eq. 1), the simultaneous estimation of both types of condition embedding leads to optimal performance for both the tokenizer-detokenizer framework and VL-GPT. We hypothesize that estimating image condition embedding enables our tokenizer to retain more pixel information from the input image, which is beneficial for image reconstruction. Meanwhile, estimating text condition embedding allows the visual embeddings to contain more high-level semantics, leading to improved performance in subsequent vision and language tasks.

5. Conclusion

We propose VL-GPT, a generative pre-trained transformer model for vision and language understanding and generation. The model incorporates an innovative image tokenizer-detokenizer framework, enabling it to be pre-trained on large-scale multimodal corpora with a unified auto-regressive objective. Upon completion of the pre-training, VL-GPT exhibits competitive performance across various academic benchmarks and manifests several appealing emergent capabilities. As for limitations, the effectiveness of our method has not been verified through the scaling up of model parameters. We hope that our work will stimulate further exploration in the pursuit of general intelligence within the multimodal research community.

References

- [1] Jean-Baptiste Alayrac, Jeff Donahue, Pauline Luc, Antoine Miech, Iain Barr, Yana Hasson, Karel Lenc, Arthur Mensch, Katherine Millican, Malcolm Reynolds, et al. Flamingo: a visual language model for few-shot learning. *Advances in Neural Information Processing Systems*, 35:23716–23736, 2022.
- [2] Hangbo Bao, Li Dong, Songhao Piao, and Furu Wei. Beit: Bert pre-training of image transformers. *arXiv preprint arXiv:2106.08254*, 2021.
- [3] Tim Brooks, Aleksander Holynski, and Alexei A Efros. Instructpix2pix: Learning to follow image editing instructions. In *Proceedings of the IEEE/CVF Conference on Computer Vision and Pattern Recognition*, pages 18392–18402, 2023.
- [4] Tom Brown, Benjamin Mann, Nick Ryder, Melanie Subbiah, Jared D Kaplan, Prafulla Dhariwal, Arvind Neelakantan, Pranav Shyam, Girish Sastry, Amanda Askell, et al. Language models are few-shot learners. *Advances in neural information processing systems*, 33:1877–1901, 2020.
- [5] Xinlei Chen, Hao Fang, Tsung-Yi Lin, Ramakrishna Vedantam, Saurabh Gupta, Piotr Dollár, and C Lawrence Zitnick. Microsoft coco captions: Data collection and evaluation server. *arXiv preprint arXiv:1504.00325*, 2015.
- [6] Yen-Chun Chen, Linjie Li, Licheng Yu, Ahmed El Kholy, Faisal Ahmed, Zhe Gan, Yu Cheng, and Jingjing Liu. Uniter: Universal image-text representation learning, 2020.
- [7] Abhishek Das, Satwik Kottur, Khushi Gupta, Avi Singh, Deshraj Yadav, José MF Moura, Devi Parikh, and Dhruv Batra. Visual dialog. In *Proceedings of the IEEE conference on computer vision and pattern recognition*, pages 326–335, 2017.
- [8] Jacob Devlin, Ming-Wei Chang, Kenton Lee, and Kristina Toutanova. Bert: Pre-training of deep bidirectional transformers for language understanding. *arXiv preprint arXiv:1810.04805*, 2018.
- [9] Runpei Dong, Chunrui Han, Yuang Peng, Zekun Qi, Zheng Ge, Jinrong Yang, Liang Zhao, Jianjian Sun, Hongyu Zhou, Haoran Wei, et al. Dreamllm: Synergistic multimodal comprehension and creation. *arXiv preprint arXiv:2309.11499*, 2023.
- [10] Alexey Dosovitskiy, Lucas Beyer, Alexander Kolesnikov, Dirk Weissenborn, Xiaohua Zhai, Thomas Unterthiner, Mostafa Dehghani, Matthias Minderer, Georg Heigold, Sylvain Gelly, et al. An image is worth 16x16 words: Transformers for image recognition at scale. *arXiv preprint arXiv:2010.11929*, 2020.
- [11] Yuying Ge, Yixiao Ge, Ziyun Zeng, Xintao Wang, and Ying Shan. Planting a seed of vision in large language model. *arXiv preprint arXiv:2307.08041*, 2023.
- [12] Yash Goyal, Tejas Khot, Douglas Summers-Stay, Dhruv Batra, and Devi Parikh. Making the v in vqa matter: Elevating the role of image understanding in visual question answering. In *Proceedings of the IEEE conference on computer vision and pattern recognition*, pages 6904–6913, 2017.
- [13] Danna Gurari, Qing Li, Abigale J Stangl, Anhong Guo, Chi Lin, Kristen Grauman, Jiebo Luo, and Jeffrey P Bigham. Vizwiz grand challenge: Answering visual questions from blind people. In *Proceedings of the IEEE conference on computer vision and pattern recognition*, pages 3608–3617, 2018.
- [14] Yaru Hao, Haoyu Song, Li Dong, Shaohan Huang, Zewen Chi, Wenhui Wang, Shuming Ma, and Furu Wei. Language models are general-purpose interfaces. *arXiv preprint arXiv:2206.06336*, 2022.
- [15] Edward J Hu, Yelong Shen, Phillip Wallis, Zeyuan Allen-Zhu, Yuanzhi Li, Shean Wang, Lu Wang, and Weizhu Chen. Lora: Low-rank adaptation of large language models. *arXiv preprint arXiv:2106.09685*, 2021.
- [16] Shaohan Huang, Li Dong, Wenhui Wang, Yaru Hao, Saksham Singhal, Shuming Ma, Tengchao Lv, Lei Cui, Owais Khan Mohammed, Qiang Liu, et al. Language is not all you need: Aligning perception with language models. *arXiv preprint arXiv:2302.14045*, 2023.
- [17] Drew A Hudson and Christopher D Manning. Gqa: A new dataset for real-world visual reasoning and compositional question answering. In *Proceedings of the IEEE/CVF conference on computer vision and pattern recognition*, pages 6700–6709, 2019.
- [18] Jing Yu Koh, Daniel Fried, and Ruslan Salakhutdinov. Generating images with multimodal language models. *arXiv preprint arXiv:2305.17216*, 2023.
- [19] Taku Kudo and John Richardson. Sentencepiece: A simple and language independent subword tokenizer and detokenizer for neural text processing. *arXiv preprint arXiv:1808.06226*, 2018.
- [20] LAION. Laion-aesthetics. <https://laion.ai/blog/laion-coco/>.
- [21] Hugo Laurençon, Lucile Saulnier, Léo Tronchon, Stas Bekman, Amanpreet Singh, Anton Lozhkov, Thomas Wang, Siddharth Karamcheti, Alexander M. Rush, Douwe Kiela, Matthieu Cord, and Victor Sanh. Obelics: An open web-scale filtered dataset of interleaved image-text documents, 2023.
- [22] Bo Li, Yuanhan Zhang, Liangyu Chen, Jinghao Wang, Jingkang Yang, and Ziwei Liu. Otter: A multi-modal model with in-context instruction tuning. *arXiv preprint arXiv:2305.03726*, 2023.
- [23] Dongxu Li, Junnan Li, and Steven CH Hoi. Blip-diffusion: Pre-trained subject representation for controllable text-to-image generation and editing. *arXiv preprint arXiv:2305.14720*, 2023.
- [24] Junnan Li, Dongxu Li, Silvio Savarese, and Steven Hoi. Blip-2: Bootstrapping language-image pre-training with frozen image encoders and large language models. *arXiv preprint arXiv:2301.12597*, 2023.
- [25] Haotian Liu, Chunyuan Li, Qingyang Wu, and Yong Jae Lee. Visual instruction tuning. *arXiv preprint arXiv:2304.08485*, 2023.
- [26] Ilya Loshchilov and Frank Hutter. Decoupled weight decay regularization. *arXiv preprint arXiv:1711.05101*, 2017.
- [27] Jiasen Lu, Christopher Clark, Rowan Zellers, Roozbeh Motlaghi, and Aniruddha Kembhavi. Unified-io: A unified model for vision, language, and multi-modal tasks. *arXiv preprint arXiv:2206.08916*, 2022.

- [28] Kenneth Marino, Mohammad Rastegari, Ali Farhadi, and Roozbeh Mottaghi. Ok-vqa: A visual question answering benchmark requiring external knowledge. In *Proceedings of the IEEE/cvf conference on computer vision and pattern recognition*, pages 3195–3204, 2019.
- [29] OpenAI. Gpt-4 technical report, 2023.
- [30] Xichen Pan, Li Dong, Shaohan Huang, Zhiliang Peng, Wenhui Chen, and Furu Wei. Kosmos-g: Generating images in context with multimodal large language models. *arXiv preprint arXiv:2310.02992*, 2023.
- [31] Alec Radford, Karthik Narasimhan, Tim Salimans, Ilya Sutskever, et al. Improving language understanding by generative pre-training. 2018.
- [32] Alec Radford, Jong Wook Kim, Chris Hallacy, Aditya Ramesh, Gabriel Goh, Sandhini Agarwal, Girish Sastry, Amanda Askell, Pamela Mishkin, Jack Clark, et al. Learning transferable visual models from natural language supervision. In *International conference on machine learning*, pages 8748–8763. PMLR, 2021.
- [33] Colin Raffel, Noam Shazeer, Adam Roberts, Katherine Lee, Sharan Narang, Michael Matena, Yanqi Zhou, Wei Li, and Peter J Liu. Exploring the limits of transfer learning with a unified text-to-text transformer. *The Journal of Machine Learning Research*, 21(1):5485–5551, 2020.
- [34] Aditya Ramesh, Prafulla Dhariwal, Alex Nichol, Casey Chu, and Mark Chen. Hierarchical text-conditional image generation with clip latents. *arXiv preprint arXiv:2204.06125*, 1(2):3, 2022.
- [35] Robin Rombach, Andreas Blattmann, Dominik Lorenz, Patrick Esser, and Björn Ommer. High-resolution image synthesis with latent diffusion models. In *Proceedings of the IEEE/CVF conference on computer vision and pattern recognition*, pages 10684–10695, 2022.
- [36] Christoph Schuhmann, Köpf, Andreas, Theo Coombes, Richard Vencu, Benjamin Trom, and Romain Beaumont. Laion coco: 600m synthetic captions from laion2b-en. <https://laion.ai/blog/laion-coco/>.
- [37] Piyush Sharma, Nan Ding, Sebastian Goodman, and Radu Soricut. Conceptual captions: A cleaned, hypernymed, image alt-text dataset for automatic image captioning. In *Proceedings of the 56th Annual Meeting of the Association for Computational Linguistics (Volume 1: Long Papers)*, pages 2556–2565, 2018.
- [38] Yongliang Shen, Kaitao Song, Xu Tan, Dongsheng Li, Weiming Lu, and Yueting Zhuang. Hugginggpt: Solving ai tasks with chatgpt and its friends in huggingface. *arXiv preprint arXiv:2303.17580*, 2023.
- [39] Quan Sun, Qiyang Yu, Yufeng Cui, Fan Zhang, Xiaosong Zhang, Yueze Wang, Hongcheng Gao, Jingjing Liu, Tiejun Huang, and Xinlong Wang. Generative pretraining in multimodality. *arXiv preprint arXiv:2307.05222*, 2023.
- [40] Hugo Touvron, Thibaut Lavril, Gautier Izacard, Xavier Martinet, Marie-Anne Lachaux, Timothée Lacroix, Baptiste Rozière, Naman Goyal, Eric Hambro, Faisal Azhar, et al. Llama: Open and efficient foundation language models. *arXiv preprint arXiv:2302.13971*, 2023.
- [41] Hugo Touvron, Louis Martin, Kevin Stone, Peter Albert, Amjad Almahairi, Yasmine Babaei, Nikolay Bashlykov, Soumya Batra, Prajjwal Bhargava, Shruti Bhosale, et al. Llama 2: Open foundation and fine-tuned chat models. *arXiv preprint arXiv:2307.09288*, 2023.
- [42] Ashish Vaswani, Noam Shazeer, Niki Parmar, Jakob Uszkoreit, Llion Jones, Aidan N Gomez, Łukasz Kaiser, and Illia Polosukhin. Attention is all you need. *Advances in neural information processing systems*, 30, 2017.
- [43] Changhan Wang, Kyunghyun Cho, and Jiatao Gu. Neural machine translation with byte-level subwords. In *Proceedings of the AAAI conference on artificial intelligence*, pages 9154–9160, 2020.
- [44] Peng Wang, An Yang, Rui Men, Junyang Lin, Shuai Bai, Zhikang Li, Jianxin Ma, Chang Zhou, Jingren Zhou, and Hongxia Yang. Ofa: Unifying architectures, tasks, and modalities through a simple sequence-to-sequence learning framework. In *International Conference on Machine Learning*, pages 23318–23340. PMLR, 2022.
- [45] Wenhui Wang, Hangbo Bao, Li Dong, Johan Bjorck, Zhiliang Peng, Qiang Liu, Kriti Aggarwal, Owais Khan Mohammed, Saksham Singhal, Subhojit Som, et al. Image as a foreign language: Beit pretraining for all vision and vision-language tasks. *arXiv preprint arXiv:2208.10442*, 2022.
- [46] Samuel Weinbach, Marco Bellagente, Constantin Eichenberg, Andrew Dai, Robert Baldock, Souradeep Nanda, Björn Deiseroth, Koen Oostermeijer, Hannah Teufel, and Andres Felipe Cruz-Salinas. M-vader: A model for diffusion with multimodal context. *arXiv preprint arXiv:2212.02936*, 2022.
- [47] Chenfei Wu, Shengming Yin, Weizhen Qi, Xiaodong Wang, Zecheng Tang, and Nan Duan. Visual chatgpt: Talking, drawing and editing with visual foundation models. *arXiv preprint arXiv:2303.04671*, 2023.
- [48] Shengqiong Wu, Hao Fei, Leigang Qu, Wei Ji, and Tat-Seng Chua. Next-gpt: Any-to-any multimodal llm. *arXiv preprint arXiv:2309.05519*, 2023.
- [49] Hu Ye, Jun Zhang, Sibor Liu, Xiao Han, and Wei Yang. Ip-adapter: Text compatible image prompt adapter for text-to-image diffusion models. *arXiv preprint arXiv:2308.06721*, 2023.
- [50] Jiahui Yu, Zirui Wang, Vijay Vasudevan, Legg Yeung, Mojtaba Seyedhosseini, and Yonghui Wu. Coca: Contrastive captioners are image-text foundation models, 2022.
- [51] Lili Yu, Bowen Shi, Ramakanth Pasunuru, Benjamin Muller, Olga Golovneva, Tianlu Wang, Arun Babu, Binh Tang, Brian Karrer, Shelly Sheynin, et al. Scaling autoregressive multimodal models: Pretraining and instruction tuning. *arXiv preprint arXiv:2309.02591*, 2023.
- [52] Lu Yuan, Dongdong Chen, Yi-Ling Chen, Noel Codella, Xiyang Dai, Jianfeng Gao, Houdong Hu, Xuedong Huang, Boxin Li, Chunyuan Li, Ce Liu, Mengchen Liu, Zicheng Liu, Yumao Lu, Yu Shi, Lijuan Wang, Jianfeng Wang, Bin Xiao, Zhen Xiao, Jianwei Yang, Michael Zeng, Luowei Zhou, and Pengchuan Zhang. Florence: A new foundation model for computer vision, 2021.
- [53] Kai Zhang, Lingbo Mo, Wenhui Chen, Huan Sun, and Yu Su. Magicbrush: A manually annotated dataset for instruction-guided image editing. *arXiv preprint arXiv:2306.10012*, 2023.

- [54] Susan Zhang, Stephen Roller, Naman Goyal, Mikel Artetxe, Moya Chen, Shuohui Chen, Christopher Dewan, Mona Diab, Xian Li, Xi Victoria Lin, et al. Opt: Open pre-trained transformer language models. *arXiv preprint arXiv:2205.01068*, 2022.
- [55] Bo Zhao, Boya Wu, and Tiejun Huang. Svit: Scaling up visual instruction tuning. *arXiv preprint arXiv:2307.04087*, 2023.
- [56] Deyao Zhu, Jun Chen, Xiaoqian Shen, Xiang Li, and Mohamed Elhoseiny. Minigt-4: Enhancing vision-language understanding with advanced large language models. *arXiv preprint arXiv:2304.10592*, 2023.
- [57] Wanrong Zhu, Jack Hessel, Anas Awadalla, Samir Yitzhak Gadre, Jesse Dodge, Alex Fang, Youngjae Yu, Ludwig Schmidt, William Yang Wang, and Yejin Choi. Multimodal c4: An open, billion-scale corpus of images interleaved with text. *arXiv preprint arXiv:2304.06939*, 2023.

Dataset	Task	Split	Metric
COCOCap	Scene Description	test	CIDEr (\uparrow)
VQAv2	Scene Understanding QA	test-dev	VQA acc. (\uparrow)
GQA	Scene Understanding QA	test-dev	VQA acc. (\uparrow)
OKVQA	External Knowledge QA	val	VQA acc. (\uparrow)
VizWiz	Scene Understanding QA	test-dev	VQA acc. (\uparrow)
VisDial	Image Dialogue	val	NDCG (\uparrow)
COCO	Text-to-Image Generation	val test	FID (\downarrow)

Table 5. Summary of the evaluation benchmarks.

6. Training Details

6.1. Training of image tokenizer and detokenizer

Datasets. The image-text pairs from CC3M, Laion-Aesthetics, and LAION-COCO are utilized for the training of our image tokenizer-detokenizer framework. Specifically, CC3M dataset comprises 3.3 million image-text pairs crawled from the Web. Both Laion-Aesthetics and LAION-COCO are subsets of the larger LAION-5B dataset. LAION-Aesthetics is characterized by its high aesthetic quality, while LAION-COCO is composed of images sampled from LAION-5B and their corresponding captions generated by existing vision-language models, *e.g.*, BLIP. Due to the efficient design of the framework, a relatively small subset of 10 million samples from these two datasets was found to be sufficient for model convergence in our experiments. Further exploration of experiments with larger datasets remains a prospect for future research. During the training process, data were randomly sampled from the mixture of these three datasets in a ratio proportional to their respective sizes.

Optimization. The visual encoder in the image tokenizer is initialized with CLIP-L, while the diffusion decoder in the image detokenizer incorporates the U-Net and VAE modules from IP-adapter Plus. These components remain frozen during the training process. The causal transformer in the image tokenizer and the transformer decoder in the image decoder are constructed using the standard transformer decoder, which consisting of 12 transformer blocks with random initialization. Each block comprises a causal self-attention layer, a cross attention layer, and a multilayer perception (MLP) layer. The causal attention layer plays a vital role in capturing causal dependencies among 1D visual continual embeddings, which is proved to be effective for further modeling in large vision-language models like Emu and SEED. In all experiments, the number of visual embedding N is set to 32 in our all experiments, and its dimension d is set to 4096. Image augmentation techniques employed in CLIP models are applied, which involve resizing the input image with its shorter side to 224 pixels and cropping the image to a fixed size of 224×224 pixels.

6.2. Pre-training of VL-GPT

Datasets. In addition to the datasets utilized for training the image tokenizer-detokenizer framework, publicly available interleaved image-text data, *i.e.*, MMC4 and OBELICS, are employed for the pre-training of our vision-language transformer. During pre-training, multimodal sequences with interleaved image-text data are obtained from these two datasets. For MMC4, the core split is used, and low-quality samples with a CLIP similarity between the image and its caption below 0.24 are filtered out. For OBELICS, a sequence comprising 512 tokens is randomly sampled based on the arrangement of image and text data within the original document. To augment the probability of procuring sequences containing multiple images, single-image sequences are discarded with a likelihood of 0.8. Throughout the training process, these two datasets maintain equivalent sampling probabilities, as do the sampling probabilities for datasets comprising image-text pairs and datasets containing interleaved image and text data.

Optimization. The large vision-language model, VL-GPT, is constructed by integrating the pre-trained language model LLaMA 7B with our image tokenizer-detokenizer framework. LoRA modules are attached to all linear layers in the vision-language transformer, with a LoRA rank of 32. An additional linear head is employed as a separate regression head to predict the subsequent visual continuous embedding for the current embedding. During multimodal pre-training, only the parameters in LoRA modules and the regression head are tuned, while all parameters of pre-trained LLaMA, image tokenizer, and image detokenizer remain frozen to reduce training costs. The data augmentation techniques used in the previous stage are also utilized in this phase.

6.3. Instruction tuning of VL-GPT

Datasets. To align the VL-GPT model with human instructions, multimodal instruction tuning is applied to the model using a combination of publicly available datasets, such as LLAVA, SVIT, MSCOCO Caption, InstructPix2Pix, and Magicbrush. All dataset are restructured into a conversational formulation, consisting of a system message followed by a single-turn or multi-turn conversation dialogue between a user and an assistant. The system message and conversational template employed in our method are presented in Tab. 6. Furthermore, the MSCOCO caption dataset is employed for both image captioning task and image generation task by altering the order of the image and its corresponding caption. The InstructPix2Pix and Magicbrush datasets are utilized for prompt-based image editing task. During instruction tuning, data in these datasets are sampled to construct a batch of data for model optimization in a ratio proportional to the dataset size.

Optimization. Instruction tuning is carried out on the pre-

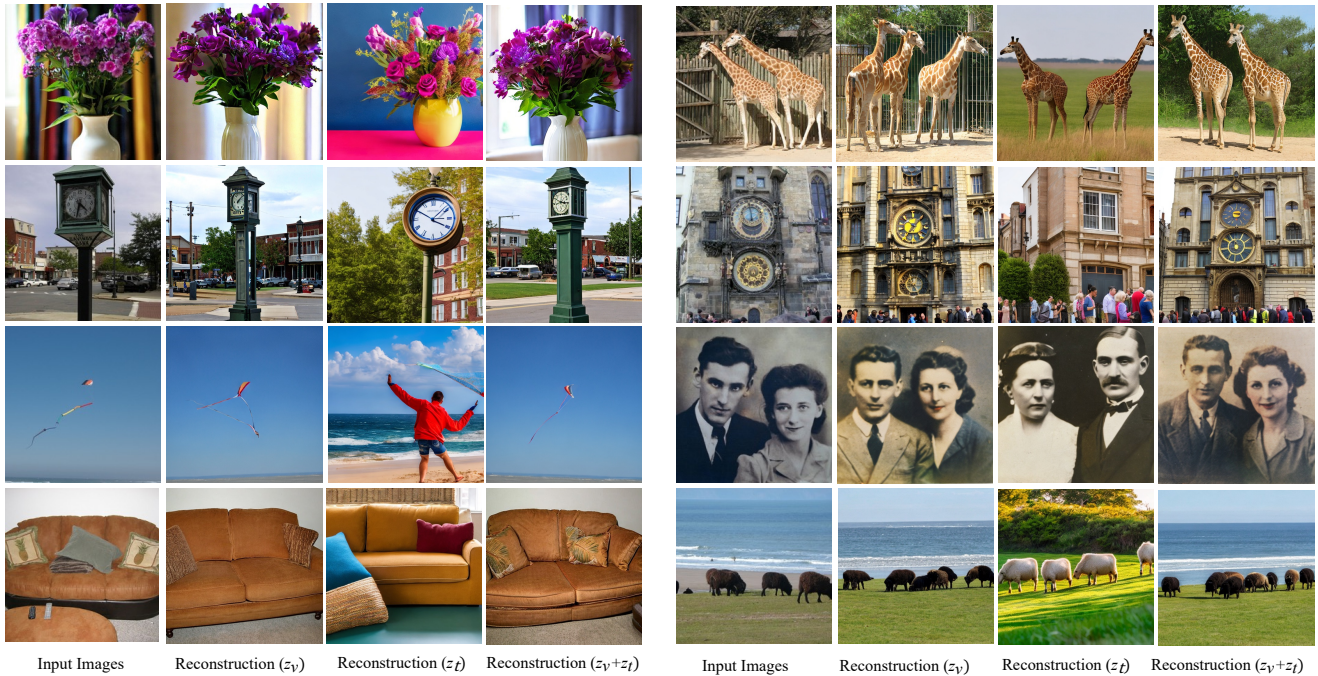


Figure 5. Reconstruction examples of our image tokenizer and detokenizer by employing different condition embedding.

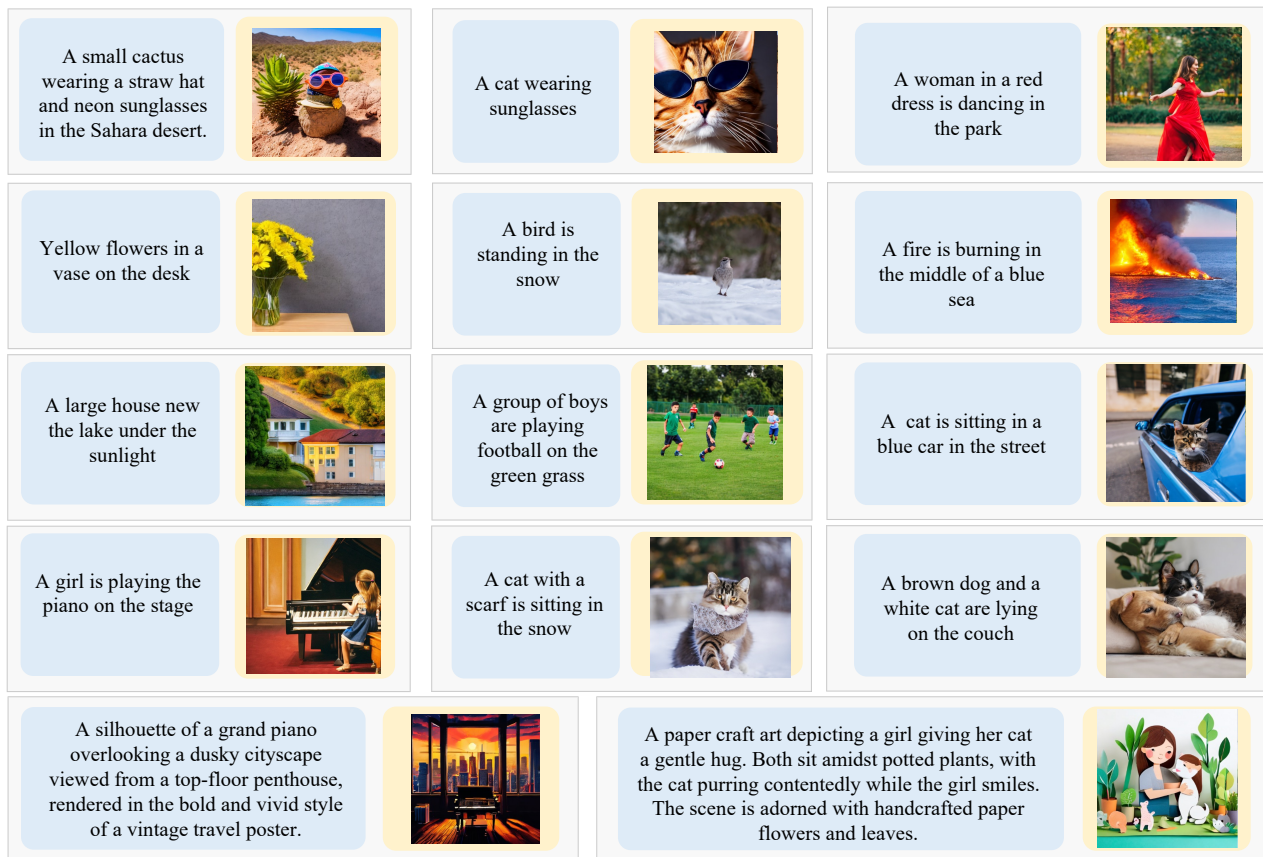


Figure 6. Examples of text-to-image generation. Blue boxes denotes the text prompt, and yellow boxes represents the generated image.

System Message		You are a helpful, respectful and honest assistant. Always answer as helpfully as possible, while being safe. Your answers should not include any harmful, unethical, racist, sexist, toxic, dangerous, or illegal content. Please ensure that your responses are socially unbiased and positive in nature.
Conversation Template	Image captioning	USER: Provide a brief description of the given image <image> ASSISTANT: <caption>.
	Image generation	USER: Create an image that visually represents the description: <caption>. ASSISTANT: Here’s the image: <image>
	Image editing	USER:<image> <editing prompt>. ASSISTANT: Here is the edited image: <image>

Table 6. Summary of prompt templates employed in instruction tuning. The notation “<image>” will be replaced with the image data. “<caption>” and “<editing prompt>” will be substituted with the corresponding caption and editing instruction, respectively.

Model	Task	Template
VL-GPT	Image captioning	<image> Please describe this image in detail in one sentence. It shows
	Image generation	An image of <caption>. [IMG]
	Image QA	<image> Based on the image, <question>? Short answer:
	Image dialog	<image> an image of <caption>. Based on the image, <question ₁ >? Short answer: <answer ₁ >. ... Based on the image, <question _n >? Short answer:
VL-GPT-I	Image captioning	USER: Provide a brief description of the given image.<image> ASSISTANT:
	Image generation	USER: Create an image that visually represents the description: <caption>. ASSISTANT:
	Image QA	USER: answer the question with the shortest answer <question>? ASSISTANT:
	Image dialog	USER: <image> ASSISTANT: an image of <caption>. USER: <question ₁ >? ASSISTANT: <answer ₁ >. ... USER: <question _n >? ASSISTANT:

Table 7. Summary of the prompting template utilized during model evaluation. The terms “<image>” and “<caption>” shall be substituted with the corresponding image and its caption. Additionally, the notations “<question_i>” and “<answer_i>” will be replaced with the *i*-th question and answer pair in the dialogue. [IMG] denotes the special token indicating the start of visual continuous embeddings.

trained VL-GPT, with the training hyper-parameters primarily following those used in the pre-training phase. As the training data for instruction tuning is significantly smaller than that employed for pre-training, the batch size is set to a smaller number, *i.e.* 512, and only four GPUs are utilized. To prevent catastrophic forgetting of the pre-trained model, the model is optimized with a reduced learning rate. Furthermore, LoRA modules are applied in the transformer model, while all other parameters remain frozen.

7. Evaluation Details

7.1. Benchmarks

To evaluate the vision and language understanding and generation ability of VL-GPT, we evaluate it on a variety of benchmarks, whose details and metrics are summarized in Tab. 5. Specifically, the test sample from any benchmark is first packaged with a task-specific prompt template and then tokenized into an incomplete multimodal sequence. Then

the VL-GPT model and its instruction tuned version, VL-GPT-I, are required to complete the multimodal sequence in an auto-regressive and open-ended manner. Evaluation results can be obtained by either using the official evaluation code or submitting our prediction on the official server. It should be noted that not all results reported in Tab. 2 are zero-shot evaluation; for instance, VL-GPT-I has been trained on COCO Caption.

7.2. Prompt Templates

To thoroughly capitalize on the knowledge acquired during pre-training while generating outputs that adhere to the style of the benchmark under evaluation, we design task-specific prompt templates for the VL-GPT and VL-GPT-I. These templates are comprehensively outlined in Tab. 7.



Figure 7. Three groups of Multimodal In-context learning. In each group, partial content in the multimodal prompts is changed, and our VL-GPT can generate desired outputs. Blue boxes represent multimodal prompts and yellow boxes indicate VL-GPT outputs.

8. Qualitative Cases

Additional reconstruction examples of our image tokenizer-detokenizer framework are illustrated in Fig. 5. Furthermore, the qualitative examples presented in Fig. 6, Fig. 7, and Fig. 8 demonstrate the superior performance of VL-GPT in various tasks, including text-to-image generation, multimodal in-context learning, and multimodal dialogue.



Please describe this image in detail.

The image features a serene lake scene with a wooden dock extending into the water. The dock is made of wood and is quite long, stretching across the entire width of the image. The water is surrounded by calm, clear water, which reflects the surrounding trees and sky.

What are the things I should be cautious about when I visit here?

When visiting this lake, you should be cautious about the weather conditions. The image shows a cloudy sky, which could indicate that it might rain or become windy. It's important to dress appropriately and bring an umbrella or a raincoat if necessary.

Can you write a poem about the image?

Sure, here's a poem about the image:
A wooden dock extends into the lake,
A place to sit and watch the world go by.
The water is calm and clear, reflecting the trees,
A serene place to sit and watch the world go by.



Describe this image in one sentence.

Two white puppies sit together on the grass

Generate image that they with pink hair

This is the generated image



Change to yellow glasses

Here is the edited image



Figure 8. Qualitative examples of multimodal dialogue by our instruction tuned VL-GPT. Blue boxes denotes the user instructions, and yellow boxes represents the assistant responses.